**Chemistry of Metals and Alloys**

*Chem. Met. Alloys* 8 (2015) 123-128
Ivan Franko National University of Lviv
www.chemetal-journal.org

# Quaternary phases $R_{1-x}Ae_xTGe_2$ ($R$ = La, Ce, Gd, Yb; $Ae$ = Ca, Sr; $T$ = Fe, Co, Ni) with $CeAl_2Ga_2$ (122) structure type

Volodymyr GVOZDETSKYI[1,2]*, Viktor HLUKHYY[2], Roman GLADYSHEVSKII[1]

[1] *Department of Inorganic Chemistry, Ivan Franko National University of Lviv, Kyryla i Mefodiya St. 6, 79005 Lviv, Ukraine*
[2] *Department of Inorganic Chemistry, Technical University of Munich, Lichtenbergstr. 4, 85747 Garching, Germany*
* *Corresponding author. Tel.: +380-32-2394506; e-mail: volodymyr.gvozdetskyi@gmail.com*

Received December 8, 2015; accepted December 30, 2015; available on-line September 19, 2016

**New quaternary phases crystallizing with the $CeAl_2Ga_2$ (*I*4/*mmm*) structure type (122 phases) were synthesized by arc melting in the *R*–*Ae*-*T*–Ge (*R* = La, Ce, Gd, Yb; *Ae* = Ca, Sr; *T* = Fe, Co, Ni) systems. The structures of $La_{0.590}Ca_{0.410}Fe_2Ge_2$ ($a$ = 4.0662(6), $c$ = 10.625(2) Å) and $La_{0.805}Sr_{0.195}Fe_2Ge_2$ ($a$ = 4.1101(2), $c$ = 10.654(1) Å) were refined on X-ray single-crystal diffraction data. Several new 122 phases were identified on X-ray powder diffraction data in the {Ce,Gd,Yb}-Ca-{Fe,Co,Ni}-Ge systems. The structures are built up from layers of rare-earth or alkaline-earth atoms, alternating with deformed [$TGe_4$] tetrahedra with tetahedral angles in the range 110° < $\alpha$ < 122° (compared to the ideal value of 109.5°). The influence of the *d*-metal and the *Ae* content on the degree of deformation of the tetrahedra is discussed.**

**Multicomponent phases / Crystal structure / $CeAl_2Ga_2$ type / X-ray powder and single-crystal diffraction**

## Introduction

Compounds crystallizing with the $CeAl_2Ga_2$ structure type (Pearson symbol *tI*10, space group *I*4/*mmm*) and known as the 122-type family of superconductive pnictides [1] are intensively investigated at present. Several substituted compounds with this structure type exhibit superconductive transitions at relatively high temperatures. For example, at atmospheric pressure the pure $CaFe_2As_2$ phase is antiferromagnetic below 170 K, but the $Ca_{1-x}Pr_xFe_2As_2$ solid solution ($0.107 < x < 0.127$) shows superconductivity below $T_c \approx 49$ K [2]. Under an applied pressure of 0.69 GPa the $CaFe_2As_2$ compound also becomes superconducting, but with a lower transition temperature, $T_c \approx 10$ K [3]. Representatives of related families are also multicomponent compounds doped with electrons or holes: *e.g.* $LaFeAsO_{1-x}F_x$ (CuZrSiAs structure type, *P*4/*nmm*, $T_c \approx 26$ K, type 1111) [4], $LiFe_{1-x}As$ (PbClF, *P*4/*nmm*, $T_c \approx 18$ K, type 111) [5], $Ca_{1-x}La_xFeAs_2$ (own structure type, *P*2, $T_c \approx 45$ K, type 112) [6], $FeSe_{1-x}$ (PbO, *P*4/*nmm*, $T_c \approx 13$ K, type 11) [7].

Over 600 compounds with 122-type structures are known in different *R*/*Ae*–*T*–*M* (*R* = rare-earth metal, *Ae* = alkaline-earth metal, *T* = transition metal, *M* = main-group element) systems [8], leading to a large number of substitution possibilities. The structures are built up from layers of deformed [$TM_4$] tetrahedra, which alternate with layers of *R* and *Ae* atoms, and, as shown in [9], the degree of deformation of the tetrahedra has a significant influence on the superconducting transition temperature. Related compounds with this structure type but without toxic arsenic, such as germanides, may also be interesting materials (*e.g.* $BaNi_2Ge_{2-x}P_x$, $SrNi_2Ge_{2-x}P_x$ are superconductors with $T_c \approx 3$ K [10,11]).

In the *Ae*–{Fe,Co,Ni}–Ge systems five compounds with 122-type structure [8,12] are known under normal conditions: $CaCo_2Ge_2$, $CaNi_2Ge_2$, $SrCo_2Ge_2$, $SrNi_2Ge_2$. and $BaCo_2Ge_2$. The $BaNi_2Ge_2$ compound has an orthorhombic structure (own structure type, *oP*20, *Pnma*, $a$ = 8.4693, $b$ = 11.3503, $c$ = 4.3212 Å) at ambient conditions, which transforms to a tetragonal one ($CeAl_2Ga_2$ type) above 753 K [13]. Isostructural $AeFe_2Ge_2$ compounds have not been observed so far. In the *R*–{Fe,Co,Ni}–Ge systems, only $EuFe_2Ge_2$ and $LuFe_2Ge_2$ are missing in the list of known compounds with 122-type structure [8]. The aim of this paper was to carry out $R_{1-x}Ae_x$ substitutions on Fe-, Co-, and Ni-based 122 germanides and investigate the influence on the structural parameters.

## Experimental details

Starting materials for the synthesis were ingots of strontium (98 %), calcium (99.5 %), lanthanum (99.9 %), cerium (99.5 %), gadolinium (99.5 %), ytterbium (99.5 %), iron (99.985 %), cobalt (99.95 %), nickel (99.97 %), and germanium (99.999 %). Quaternary alloys with a mass of 0.5 g were synthesized in an arc furnace equipped with a water-cooled copper hearth, using a tungsten electrode under argon atmosphere. The obtained pellets were re-melted three times in order to ensure homogeneity.

The alloys were homogenized in evacuated silica tubes at 673 K for 672 h in a Vulcan A-550 furnace with an automatic temperature control of ±1-2 K. The annealed alloys were quenched in cold water without breaking the ampoules. A special heat treatment procedure was performed for the alloys $La_{1-x}\{Ca,Sr\}_xFe_2Ge_2$, in order to grow single crystals suitable for diffraction studies. The alloys were enclosed in evacuated silica tubes, which were placed in a resistance furnace (Nabertherm P330). The samples were first heated to 1370 K over 6 h and held at that temperature for 2 h. Then, the temperature was lowered at a rate of 0.1 K $h^{-1}$ to 1070 K and maintained for 96 h. The samples were finally cooled to room temperature by switching off the furnace. Well-shaped single crystals were selected for further examination.

Single-crystal intensity data were collected on a STOE IPDS II-T image plate diffractometer (graphite monochromator, Mo $K\alpha$ radiation, $\lambda$ = 0.71073 Å). A numerical absorption correction was applied [14,15]. Final refinements of the structures were performed with anisotropic displacement parameters for all the atoms (SHELXL-97 [16]). The single crystals investigated on the diffractometer were analyzed with a Jeol SEM 5900LV scanning electron microscope.

X-ray phase and structural analyses were performed using diffraction data obtained on DRON-4.07 (Fe $K\alpha$ radiation, $\lambda$ = 1.93609 Å) and STOE Stadi P (Cu $K\alpha_1$ radiation, $\lambda$ = 1.54051 Å) powder diffractometers. For the indexation of the experimental diffraction patterns, theoretical patterns were calculated using the WinXPOW program package [17]. Crystal structure refinements by the Rietveld method were performed using the FullProf program [18].

## Results and discussion

Compounds of composition $CaFe_2Ge_2$ and $SrFe_2Ge_2$ do not form at ambient pressure, but the $LaFe_2Ge_2$ compound crystallizes with a $CeAl_2Ga_2$-type structure ($a$ = 4.1059, $c$ = 10.562 Å) [19]. The La atoms can be partially replaced by alkaline-earth atoms (Ca/Sr), retaining the tetragonal 122-type structure. Experimental details and crystallographic data of the two new quaternary phases, refined as $La_{0.590(7)}Ca_{0.410(7)}Fe_2Ge_2$ ($a$ = 4.0662(6), $c$ = 10.625(2) Å) and $La_{0.805(2)}Sr_{0.195(2)}Fe_2Ge_2$ ($a$ = 4.1101(2), $c$ = 10.654(1) Å), are compiled in Tables 1 and 2. The nominal compositions of the alloys, the compositions from the refinements on single-crystal data, and the compositions from EDX analyses, are in good agreement. The same is true for the cell parameters refined on powder and single-crystal data.

**Table 1** Experimental details (single-crystal data) and crystallographic data for $La_{0.590(7)}Ca_{0.410(7)}Fe_2Ge_2$ and $La_{0.805(2)}Sr_{0.195(2)}Fe_2Ge_2$ phases (cell parameters refined from powder data are given in square brackets).

| | | | |
|---|---|---|---|
| Empirical formula | | $La_{0.590(7)}Ca_{0.410(7)}Fe_2Ge_2$ | $La_{0.805(2)}Sr_{0.195(2)}Fe_2Ge_2$ |
| EDX | | La12(2)Ca8(1)Fe40(6)Ge40(9) | La17(4)Sr3(1)Fe42(7)Ge38(9) |
| Molar mass $M_r$ | | 356.26 | 385.53 |
| Space group, $Z$ | | *I*4/*mmm*, 2 | *I*4/*mmm*, 2 |
| Cell parameters: | $a$, Å | 4.0662(6) [4.0708(1)] | 4.1101(2) [4.1151(2)] |
| | $c$, Å | 10.625(2) [10.6270(4)] | 10.654(1) [10.6371(2)] |
| | $V$, Å$^3$ | 175.67(5) [176.10(2)] | 179.98(3) [180.13(2)] |
| Absorption coefficient $\mu$, mm$^{-1}$ | | 32.443 | 36.337 |
| Range of $\theta$, ° | | 3.84-29.99 | 3.82-32.44 |
| Range of $h$, $k$, $l$ | | ±5, ±5, ±14 | ±6, ±6, ±16 |
| $F$(000) | | 338 | 316 |
| Crystal size, mm | | 0.06 × 0.06 × 0.03 | 0.08 × 0.06 × 0.04 |
| Measured reflections | | 1854 | 1926 |
| Independent reflections | | 102 ($R_{int}$ = 0.095) | 125 ($R_{int}$ = 0.040) |
| Reflections with $F > 2\sigma(F)$ | | 78 ($R_\sigma$ = 0.032) | 105 ($R_\sigma$ = 0.020) |
| Number of parameters | | 10 | 10 |
| *Goof* for $F^2$ | | 1.199 | 1.193 |
| Final $R$-indices [$F > 2\sigma(F)$] | | $R1$ = 0.037, $wR2$ = 0.031 | $R1$ = 0.026, $wR2$ = 0.047 |
| $R$-indices (all data) | | $R1$ = 0.022, $wR2$ = 0.028 | $R1$ = 0.021, $wR2$ = 0.046 |
| Residual electron density, e/Å$^3$ | | 0.67 / -1.42 | 3.38 / -3.81 |

The distances between the Fe atoms in the *ab* plane, and between the Ge atoms along the *c* direction, in the $La_{0.590}Ca_{0.410}Fe_2Ge_2$ phase ($d_{Fe-Fe}$ = 2.8752(3), $d_{Ge-Ge}$ = 2.686(1) Å) are shorter than the corresponding distances in the ternary $LaFe_2Ge_2$ compound ($d_{Fe-Fe}$ = 2.903 Å, $d_{Ge-Ge}$ = 2.706 Å). On the contrary, in the $La_{0.805}Sr_{0.195}Fe_2Ge_2$ phase the corresponding interatomic distances ($d_{Fe-Fe}$ = 2.9063(1), $d_{Ge-Ge}$ = 2.741(2) Å) are slightly longer (Fig. 1). The structures of the quaternary phases are built up from less deformed [$FeGe_4$] tetrahedra than the ternary phase.

**Table 2** Atomic coordinates and displacement parameters for $La_{0.590(7)}Ca_{0.410(7)}Fe_2Ge_2$ and $La_{0.805(2)}Sr_{0.195(2)}Fe_2Ge_2$.

| $La_{0.590(7)}Ca_{0.410(7)}Fe_2Ge_2$ ($CeAl_2Ga_2$, *tI*10, *I*4/*mmm*, *a* = 4.0662(6), *c* = 10.625(2) Å) | | | | | | |
|---|---|---|---|---|---|---|
| Atom | Wyckoff position | Occupancy | *x* | *y* | *z* | $U_{eq} \times 10^2$, Å$^2$ |
| La/Ca | 2*a* | 0.590(7)/0.410(7) | 0 | 0 | 0 | 0.65(3) |
| Fe | 4*d* | 1 | 0 | ½ | ¼ | 0.78(3) |
| Ge | 4*e* | 1 | 0 | 0 | 0.37361(8) | 0.78(3) |
| $La_{0.805(2)}Sr_{0.195(2)}Fe_2Ge_2$ ($CeAl_2Ga_2$, *tI*10, *I*4/*mmm*, *a* = 4.1101(2), *c* = 10.654(1) Å) | | | | | | |
| Atom | Wyckoff position | Occupancy | *x* | *y* | *z* | $U_{eq} \times 10^2$, Å$^2$ |
| La/Sr | 2*a* | 0.805(2)/0.195(2) | 0 | 0 | 0 | 0.97(3) |
| Fe | 4*d* | 1 | 0 | ½ | ¼ | 1.08(4) |
| Ge | 4*e* | 1 | 0 | 0 | 0.37136(11) | 1.00(3) |

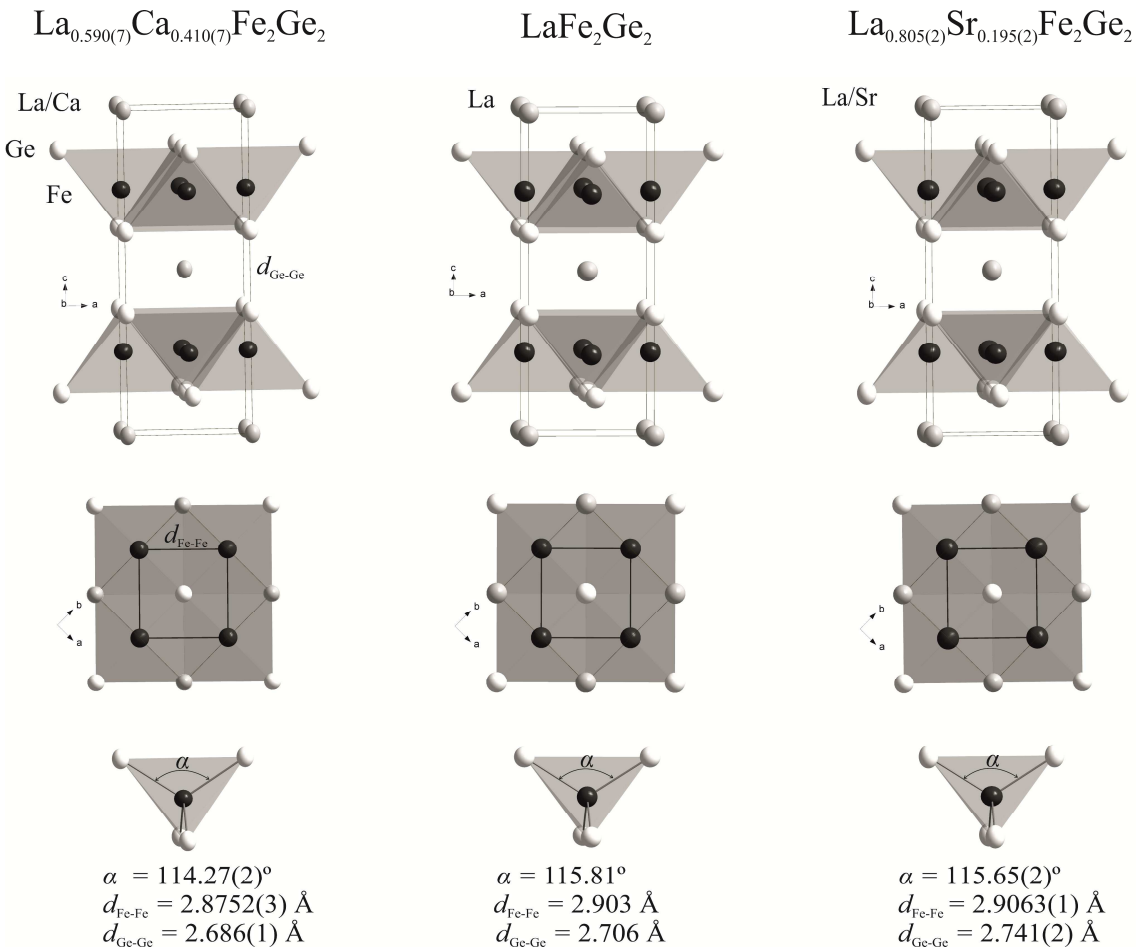


**Fig. 1** Crystal structures of the quaternary 122 phases $La_{0.590(7)}Ca_{0.410(7)}Fe_2Ge_2$ and $La_{0.805(2)}Sr_{0.195(2)}Fe_2Ge_2$, comparing with the ternary compound $LaFe_2Ge_2$.

Several new isostructural phases were synthesized in the {Ce,Gd,Yb}–Ca–{Fe,Co,Ni}–Ge quaternary systems (preliminary data in [20]). The crystal structure refinements showed the formation of solid solutions with the composition ranges and cell parameters listed in Table 3. The values of the unit-cell parameters of these phases are comparable to those of the isotypic compounds in the corresponding ternary systems: $CeFe_2Ge_2$ ($a$ = 4.0713, $c$ = 10.483 Å) [21,22], $CeCo_2Ge_2$ ($a$ = 4.071, $c$ = 10.170 Å) [21], $CeNi_2Ge_2$ ($a$ = 4.150, $c$ = 9.854 Å) [21], $GdFe_2Ge_2$ ($a$ = 3.9867, $c$ = 10.4798 Å) [21,23], $GdCo_2Ge_2$ ($a$ = 3.996, $c$ = 10.066 Å) [21], $GdNi_2Ge_2$ ($a$ = 4.063, $c$ = 9.783 Å) [21], $YbFe_2Ge_2$ ($a$ = 3.924, $c$ = 10.503 Å) [24], $YbCo_2Ge_2$ ($a$ = 3.9311, $c$ = 10.040 Å) [25], $YbNi_2Ge_2$ ($a$ = 4.001, $c$ = 9.733 Å) [21], $CaCo_2Ge_2$ ($a$ = 3.99, $c$ = 10.298 Å) [19], and $CaNi_2Ge_2$ ($a$ = 4.0749, $c$ = 9.987 Å) [19]. Within each solid solution, the $c$-parameter of the tetragonal $CeAl_2Ga_2$-type phase increases with increasing Ca content (Fig. 2). The $a$-parameter decreases with increasing Ca content when $R$ = Ce, increases when $R$ = Yb, and remains nearly the same when $R$ = Gd. The replacement Fe→Co→Ni decreases the $c$-parameter and increases the $a$-parameter. As noted earlier, the main motifs of these structures are layers containing edge-sharing [$T$Ge$_4$] tetrahedra, parallel to the $ab$ plane and separated by $R$/$Ae$ atoms. It can be seen from Table 3 that the cell dimensions of the new 122-phases cover a wide range of values. These can be related to the deviation of the central angle of the [$T$Ge$_4$] tetrahedra from the ideal value of 109.5°, shown in the last column of the table. In the structures of the phases studied here, this angle, $\alpha$ = Ge-$T$-Ge, varies within the range 110° < $\alpha$ < 122°. Taking into consideration the fact that superconductive behavior in similar compounds (several types of iron-based superconductors have been identified in the recent years, the most prominent being the 1111, 122, 111, and the 11 families mentioned above) has been related to the value of $\alpha$, the new 122-phases offer a possibility to tune the superconductive properties. The Co-based phases are built up of less deformed [$T$Ge$_4$] tetrahedra, compared to the Fe- or Ni-based phases.

The choice of the $d$-metal (Fe, Co or Ni) has a significant influence on the structural parameters of the 122 phases. This arises from the increasing number of electrons in the $d$-orbitals in the row Fe→Co→Ni. The additional electrons provided by Co [$3d^7 4s^2$] and Ni [$3d^8 4s^2$] with respect to Fe [$3d^6 4s^2$] would have to occupy anti-bonding bands [26-28], and therefore the interatomic distances between $d$-metal atoms must increase, as can be seen in Fig. 2 (the shortest distances between $T$ atoms are proportional to the $a$-parameter of the unit cell, $d_{T\text{-}T} = a/\sqrt{2}$). The [$T$Ge$_4$] tetrahedra exhibit broadening in the $ab$ plane, which is accompanied by compression along the $c$-direction and, therefore, decrease of the $c$-parameter. As a consequence, the degree of deformation of the tetrahedra increases in the row $\alpha$[FeGe$_4$] < $\alpha$[CoGe$_4$] < $\alpha$[NiGe$_4$]. Substitution of Ca for La in the ternary $LaFe_2Ge_2$ compound results in reduced electron concentration in the $R_{1-x}Ae_x$ layers (Ca [$4s^2$] compared with La [$5d^1 6s^2$]), which will also influence the bonding in the [$T$Ge$_4$] tetrahedra. In agreement with the reasoning made above, the [FeGe$_4$] tetrahedra in $La_{0.590}Ca_{0.410}Fe_2Ge_2$ ($\alpha$ = 114.27°) are less deformed than those in $LaFe_2Ge_2$ ($\alpha$ = 115.81°), the difference being ~1.5°. A similar effect is expected in the case of the Sr-substituted phase $La_{0.805}Sr_{0.195}Fe_2Ge_2$ ($\alpha$ = 115.65°). Here, however, the considerably larger Sr atoms (size factor) have an opposite influence on the structure, and the result is a limited decrease of ~0.15° for the $\alpha$-angle. Within the row Ce [$4f^1 5d^1 6s^2$] → Gd [$4f^7 5d^1 6s^2$] → Yb [$4f^{14} 5d^0 6s^2$] the valence electron concentration decreases. Therefore, the strongest electron effect (which causes a reduction of the $\alpha$-angle in the [$T$Ge$_4$] tetrahedra) due to the substitution of Ca for $R$ atoms is observed for the Ce-containing phases (see Fig. 2). The decrease of the tetrahedral $\alpha$-angle in the structures of the Gd-containing phases is less sharp than for the Ce-containing ones. When $R$ = Yb, no decrease of the electron concentration is achieved, but, over against due to increasing ionic interaction between the [$Yb_{1-x}Ca_x$] and [$T$Ge$_4$] layers, the electron concentration in the tetrahedra may slightly increase, which would explain that the [$T$Ge$_4$] tetrahedra in the

**Table 3** Solid solutions with $CeAl_2Ga_2$-type structure in the quaternary systems {Ce,Gd,Yb}–Ca–{Fe,Co,Ni}–Ge: composition range, cell parameters and tetrahedral angle ($\alpha$).

| System | $x$ | $a$, Å | $c$, Å | $\alpha$, ° |
|---|---|---|---|---|
| $Ce_{1-x}Ca_xFe_2Ge_2$ | 0.116(7)-0.797(9) | 4.06666(9)-4.0063(2) | 10.5034(3)-10.6553(7) | 113.76(5)-111.7(1) |
| $Ce_{1-x}Ca_xCo_2Ge_2$ | 0.18(1)-0.792(9) | 4.06009(9)-4.0066(2) | 10.2009(3)-10.2930(7) | 118.64(4)-115.1(1) |
| $Ce_{1-x}Ca_xNi_2Ge_2$ | 0.099(5)-0.882(6) | 4.14955(8)-4.0870(1) | 9.8606(2)-9.9777(5) | 121.47(4)-118.88(9) |
| $Gd_{1-x}Ca_xFe_2Ge_2$ | 0.043(5)-0.472(6) | 3.98615(7)-3.9877(1) | 10.4934(2)-10.5675(3) | 112.78(4)-111.94(4) |
| $Gd_{1-x}Ca_xCo_2Ge_2$ | 0.075(8)-0.900(4) | 3.99269(5)-3.9879(1) | 10.0913(2)-10.2952(4) | 116.52(4)-116.19(7) |
| $Gd_{1-x}Ca_xNi_2Ge_2$ | 0.106(4)-0.837(4) | 4.06737(7)-4.0795(2) | 9.8122(2)-9.9597(5) | 119.62(4)-119.0(1) |
| $Yb_{1-x}Ca_xFe_2Ge_2$ | 0.246(7)-0.696(2) | 3.94199(8)-3.97196(9) | 10.5428(3)-10.6436(3) | 110.48(5)-111.40(4) |
| $Yb_{1-x}Ca_xCo_2Ge_2$ | 0.31(1)-0.755(4) | 3.9492(5)-3.9821(2) | 10.1112(7)-10.2439(6) | 114.34(8)-115.68(8) |
| $Yb_{1-x}Ca_xNi_2Ge_2$ | 0.281(3)-0.755(1) | 4.02544(7)-4.06357(7) | 9.8411(3)-9.9537(2) | 118.22(4)-118.4(1) |

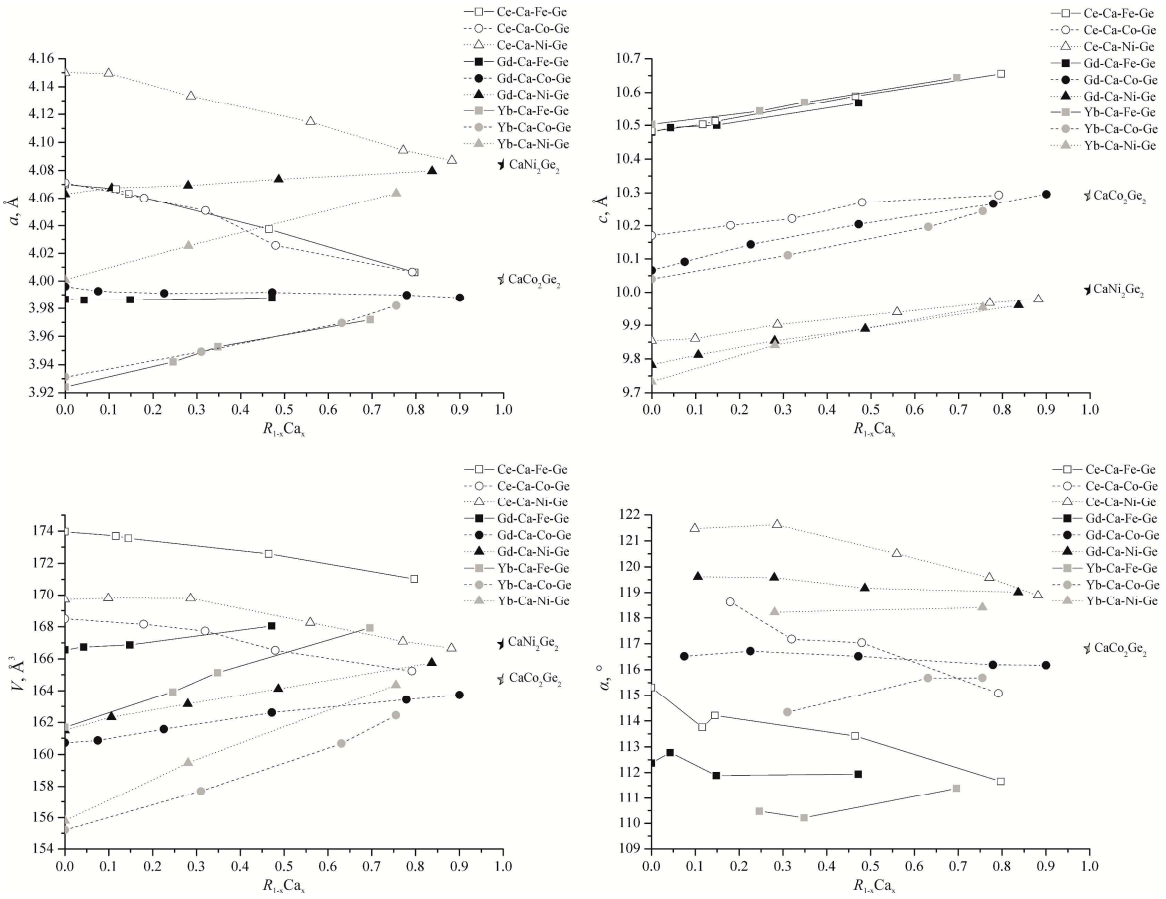


**Fig. 2** Cell parameters and $\alpha$-angles inside the [$T$Ge$_4$] tetrahedra in the structures of the phases with CeAl$_2$Ga$_2$-type structures in the quaternary systems {Ce,Gd,Yb}–Ca–{Fe,Co,Ni}–Ge.

$Yb_{1-x}Ca_xT_2Ge_2$ phases become more deformed with increasing Ca content. The significance of the electronic factor has been confirmed by the replacement of four-valent Ge by five-valent Sb in the 122-homologues $EuNi_{2-x}Sb_2$ and $SrNi_{2-x}Sb_2$ [27,29]. The substitution leads to an unusual increase of the electron concentration in the [NiSb$_4$] tetrahedra, which is compensated by Ni defects.

## Conclusions

*Ae*–*T*–*Pn* (*Ae* = alkaline-earth element; *T* = transition metal; *Pn* = pnictogen) systems are intensively investigated because of the existence of superconductors with 122 composition and CeAl$_2$Ga$_2$-type structure. These phases may show superconductive transitions at relatively high temperatures, which can be related to the value of the $\alpha$-angle, *i.e.* the *Pn*-*T*-*Pn* angle at the center of the [$TPn_4$] tetrahedra. The new homologue phases $R_{1-x}Ae_xTGe_2$ ($R$ = La, Ce, Gd, Yb; $Ae$ = Ca, Sr, $T$ = Fe, Co, Ni) cover a wide range of values of the tetrahedral angle ($110° < \alpha < 122°$), depending on the type of *d*-metal and the *R*/*Ae* content. The value of the $\alpha$-angle increases within the row $\alpha$[FeGe$_4$] < $\alpha$[CoGe$_4$] < $\alpha$[NiGe$_4$], because of the increase of the number of electrons in anti-bonding bands. Similarly, substitution of Ca atoms for the *R* atoms decreases the $\alpha$-angle when the number of valence electrons in the $4f^n5d^m6s^2$ configuration is larger than for the Ca atoms (for $R$ = La, Ce, Gd). There is no difference in the case where $R$ = Yb [$4f^{14}5d^06s^2$] and the slightly larger deformation observed with increasing Ca content may here be due to ionic interactions between the [$Yb_{1-x}Ca_x$] atoms and the [$T$Ge$_4$] tetrahedra .

## Acknowledgements

This work was supported by the Ministry of Education and Sciences of Ukraine under the grant No. 0115U003257, and by the Deutscher Akademischer Auslandsdienst for a research stipend (V.G.) at the Technical University of Munich (grant No. A/12/85156).

**References**


[1] K. Ishida, Y. Nakai, H. Hosono, *J. Phys. Soc. Jpn.* 78/6 (2009) 062001 (20 p).

[2] B. Lv, L. Deng, M. Gooch, F. Wei, Y. Sun, J.K. Meen, Y. Xue, B. Lorenz, C. Chu, *Proc. Natl. Acad. Sci. U.S.A.* 108/38 (2011) 15705-15709.

[3] T. Park, E. Park, H. Lee, T. Klimczuk, E.D. Bauer, F. Ronning, J.D. Thompson, *J. Phys.: Condens. Matter* 20 (2008) 322204 (3 p).

[4] Y. Kamihara, T. Watanabe, M. Hirano, H. Hosono, *J. Am. Chem. Soc.* 130 (2008) 3296-3297.

[5] X.C. Wang, Q.Q. Liu, Y.X. Lv, W.B. Gao, L.X. Yang, R.C. Yu, F.Y. Li, C.Q. Jin, *Solid State Commun.* 148 (2008) 538-540.

[6] N. Katayama, K. Kudo, S. Onari, T. Mizukami, K. Sugawara, Y. Sugiyama, Y. Kitahama, K. Iba, K. Fujimura, N. Nishimoto, M. Nohara, H. Sawa, *J. Phys. Soc. Jpn.* 82 (2013) 123702 (4 p).

[7] S. Margadonna, Y. Takabayashi, M.T. McDonald, K. Kasperkiewic, Y. Mizuguchi,Y. Takano, A.N. Fitch, E. Suard, K. Prassides, *Chem. Commun.* 43 (2008) 5607-5609.

[8] P. Villars, K. Cenzual (Eds.), *Pearson's Crystal Data. Crystal Structure Database for Inorganic Compounds*, Release 2013/14, ASM International, Materials Park (OH), 2013.

[9] ZA.. Ren, G.C. Che, X.L. Dong, J. Yang, W. Lu, W. Yi, X.L. Shen, Z.C. Li, L.L. Sun, F. Zhou and Z.X. Zhao, *EPL* 83 (2008) 17002 (4 p).

[10] D. Hirai, F. von Rohr, R.J. Cava, *Phys. Rev. B* 86 (2012) 100505(R) (5 p).

[11] V. Hlukhyy, A.V. Hoffmann, V. Grinenko, J. Scheiter, F. Hummel, D. Johrendt, T.F. Fässler, *Phys. Status Solidi B: Basic Solid State Phys.* (submitted).

[12] L. Siggelkow, V. Hlukhyy, T.F. Fässler, *Z. Anorg. Allg. Chem.* 636 (2010) 378.

[13] V. Hlukhyy, A. Hoffmann, T.F. Fässler, *Z. Anorg. Allg. Chem.* 638 (2012) 1619.

[14] *X-RED* (1.26), *Data Reduction Program*, STOE & Cie, Darmstadt, Germany, 2004.

[15] *X-SHAPE* (2.05), *Crystal Optimization for Numerical Absorption Correction*, STOE & Cie, Darmstadt, Germany, 2004.

[16] G.M. Sheldrick, *Acta Crystallogr. A* 64 (2008) 112-122.

[17] *STOE WinXPow* 3.0.2.1, STOE & Cie GmbH, Darmstadt, Germany, 2011.

[18] J. Rodriguez-Carvajal, *IUCr Newsletter.* 26 (2001) 12-29.

[19] G. Venturini, B. Malaman, *J. Alloys Compd.* 235 (1996) 201-209.

[20] V. Gvozdetskyi, R. Gladyshevskii, *Coll. Abstr. XII Int. Conf. Cryst. Chem. Intermet. Compd.*, Lviv, 2013, p. 191.

[21] W. Rieger, E. Parthé, *Monatsh. Chem.* 100 (1969) 444-454.

[22] V. Gvozdetskyi, N. German, R. Gladyshevskii, *Visn. Lviv. Univ. Ser. Khim.* 54 (2013) 11-18.

[23] V. Gvozdetskyi, N. German, R. Gladyshevskii, *Visn. Lviv. Univ. Ser. Khim.* 53 (2012) 12-19.

[24] D. Rossi, R. Marazza, R. Ferro, *J. Less-Common Met.* 58 (1978) 203-207.

[25] O.L. Sologub, P.S. Salamakha, G. Bocelli, S. Otani, T. Takabatake, *J. Alloys Compd.* 312 (2000) 196-200.

[26] W. Jeitschko, M. Reehuis, *J. Phys. Chem. Solids.* 48/7 (1987) 667-673.

[27] W.K. Hofmann, W. Jeitschko, *J. Less-Common Met.* 138 (1988) 313-322.

[28] C. Zheng, R. Hoffmann, *J. Solid State Chem.* 72 (1988) 58-71.

[29] V. Gvozdetskyi, V. Hlukhyy, T.F. Fässler, R. Gladyshevskii, *Z. Anorg. Allg. Chem.* 641/11 (2015) 1859-1862.